Bioorganic & Medicinal Chemistry 17 (2009) 6491–6495

Contents lists available at ScienceDirect

Bioorganic & Medicinal Chemistry

journal homepage: www.elsevier.com/locate/bmc

Inhibition of ribonuclease A by nucleoside–dibasic acid conjugates

Joy Debnath, Swagata Dasgupta *, Tanmaya Pathak *

Department of Chemistry, Indian Institute of Technology, Kharagpur, Kharagpur 721 302, India

ARTICLE INFO

Article history:
Received 17 June 2009
Revised 7 August 2009
Accepted 11 August 2009
Available online 14 August 2009

Keywords:
Ribonuclease A
Nucleoside–dibasic acid conjugates
Inhibition

ABSTRACT

We report the inhibition of the ribonucleolytic activity of ribonuclease A (RNase A) by nucleoside–dibasic acid conjugates for the first time. Agarose gel and precipitation assays show that the spacer length and the pK_a of the carboxylic group have an important role in the inhibitory capacity. Kinetic experiments indicate a competitive mode of inhibition with inhibition constant (K_i) value of 132 ± 3 μM for **Oxa-aT**. Docking studies revealed that the carboxylic group of the most active compounds is within hydrogen bonding distance of His-12, Lys-41 and His-119.

1. Introduction

Ribonuclease A (RNase A) is one of the most important members of the ribonuclease superfamily,[1,2] which exhibits a cytotoxic effect.[3] It adsorbs specifically to certain cells, enters the cytosol, degrades the RNA and consequently inhibits protein synthesis causing cell death. Certain pathological conditions like malignancies and infectious diseases[4] are directly linked with the ribonucleolytic activity[5] of specific members of this superfamily. These pathological diseases in addition to its cytotoxicity has triggered research in the area of inhibition of RNase A by low molecular weight compounds.[6] The ribonucleolytic center of RNase A is comprised of multiple subsites which bind the phosphate, nucleobase, and sugar components of RNA.[7,8] The main subsite is the P_1 subsite where cleavage of the phosphodiester bond occurs. His-12, Lys-41 and His-119 serve as the catalytic residues at the P_1 subsite (Fig. 1). The B_1 and B_2 sites are recognition sites for the nucleobases of the corresponding nucleotide residues. In general the B_1 and B_2 sites show pyrimidine and purine specificity, respectively.[9]

A large number of phosphate or pyrophosphate based nucleotidic inhibitors[8,9] have reported good anti-RNase A activities.[6] However, the polyionic nature of these nucleotide-based inhibitors hinders their transport through the cell membrane.[10] In earlier studies, we have demonstrated that 3′-alkylamino-3′-deoxy arauridines,[11,12] and 5′-alkylamino-5′-deoxy-uridines and thymidines efficiently inhibited RNase A,[13] where we found that the carboxylic group directly interacted with the active site histidine residues. Similar inhibitory activities were also observed for nucleobase catechin/epicatechin chimeric molecules.[14]

In this study, we have synthesized a series of dibasic acid conjugates which are actually 'monobasic' compounds because one of the –COOH groups of the dibasic acid is part of the amide bond with a free amino group in the molecule. The amide group along

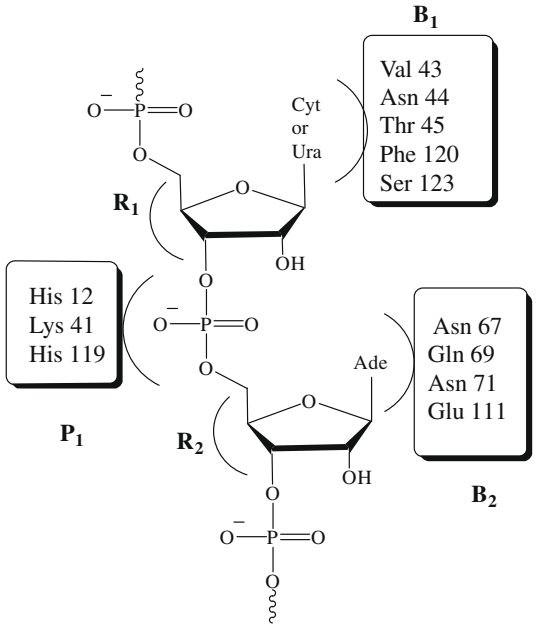

Figure 1. Active site residues of RNase A.

* Corresponding authors. Tel.: +91 3222 283306; fax: +91 3222 255303 (S.D.); tel.: +91 3222 283342 (T.P.).
E-mail addresses: swagata@chem.iitkgp.ernet.in (S. Dasgupta), tpathak@chem.iitkgp.ernet.in (T. Pathak).

0968-0896/$ - see front matter © 2009 Elsevier Ltd. All rights reserved.
doi:10.1016/j.bmc.2009.08.018

with the methylene groups attached to it act as linkers of different lengths for delivering the –COOH group to the active site. We understand that other factors including transport across membranes, metabolism etc. will be important in vivo. This is a matter of further investigation. Thus we have designed nucleoside-based inhibitors with lower ionic character compared to reported phosphate inhibitors[15] but with a capacity to ionize in biological systems. The notion is to deliver a carboxylic group to the P_1 site of the enzyme through spacers of different chain length. Electrostatic interactions present due to the ionized carboxylic group with the active site histidine residues of RNase A ought to disrupt the local acid-base equilibrium by electrostatic interactions.[16] The extent of electrostatic interactions is expected to vary with the changing pK_a values of the residual carboxylic acid moiety. Increase in chain length between the two carboxylic acid groups of the dibasic acid would also help in identifying the role of the spacer length in inhibition. Apart from this, an alternation of the hydrophobic character in the dibasic acid part can help us estimate the hydrophobic tolerance in RNase A inhibition.

2. Results and discussion

2.1. Chemistry

In order to synthesize the targeted conjugates, the known 3′-amino-2′,3′-dideoxy-5′-*O*-trityl thymidine **1**[17,18] was either reacted with diesters or anhydrides. Thus compound **1** on reactions with diethyl oxalate[19] and diethyl malonate[18] at elevated temperature followed by hydrolysis of the products under basic conditions and detritylation afforded compounds **2** and **3**, respectively, with moderate yields. On the other hand, **1** was reacted with succinic anhydride[20] and glutaric anhydride in the presence of Et_3N at room temperature to generate the partially protected conjugates **4** and **5**, respectively. Compounds **4** and **5** were detritylated to afford **6** and **7**, respectively, in good overall yields (Scheme 1). Compounds **2**, **3**, **6** and **7** were unambiguously characterized by spectral and analytical data.

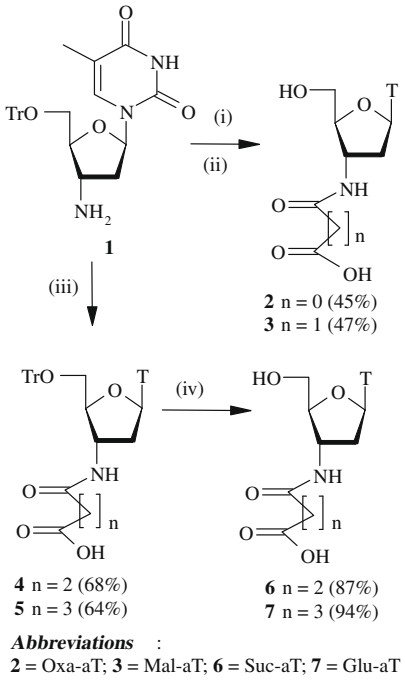

Scheme 1. Reagents and conditions: for compound **2**: (i) diethyl oxalate, 110 °C, 3 h; (ii) NaOH 4 N, refluxed for 2 h, 37% aq HCl; for compound **3**: (i) diethyl malonate, 150 °C, 3 h; (ii) NaOH 4 N, refluxed for 2 h, 37% aq HCl; for compound **4**: (iii) succinic anhydride, Et_3N, DCM, rt, 12 h; for compound **5**: (iii) glutaric anhydride, Et_3N, DCM, rt, 12 h; for compounds **6** and **7**; (iv) 20% TFA in DCM, rt, 2 h.

2.2. Enzymatic activity

The inhibition of the ribonucleolytic activity of RNase A was initially checked qualitatively by an agarose gel-based assay, where the degradation of tRNA by RNase A was monitored (Fig. 2). The most intense band observed in lane 1 for each gel is due to the presence of the control tRNA. The maximum possible degradation of tRNA by RNase A results in the faint intensity of the band observed in lane 2. The differential intensity of bands in lanes 3 to 5 indicated the extent of RNase A inhibition by the compounds at three different concentrations (lower to higher concentrations, respectively). These results qualitatively show better inhibition potency for **Oxa-aT** (**2**), **Mal-aT** (**3**), **Suc-aT** (**6**), compared to **Glu-aT** (**7**).

The histogram (Fig. 3) of relative ribonucleolytic activities obtained from a precipitation assay at a particular inhibitor concentration (1 mM) gave us a quantitative idea about the comparative inhibitory efficacy of the nucleoside–dibasic acid conjugates.

It was observed that **Oxa-aT** showed the most potent inhibition of RNase A. An increase in the chain length of the dibasic acid part resulted in a weaker inhibition with that for **Glu-aT** being quite low. This suggests that the distance between the 'free carboxylic group' and the nucleoside moiety plays a decisive role in the ribonuclease inhibition process. The comparative bar diagram for the residual ribonucleolytic activity of RNase A obtained from the agarose gel (quantified by individual band analysis) and precipitation assays is shown in Figure 4. It showed same trend of inhibitory activity on RNase A.

To determine the nature of inhibition and the corresponding inhibition constants, kinetic experiments were conducted with the synthesized compounds. The inhibition constant values(K_i) obtained for **Oxa-aT**, **Mal-aT** and **Suc-aT** were 132 ± 3, 380 ± 2 and 918 ± 2 μM, respectively. The nature of the Dixon plots for **Oxa-aT**, **Mal-aT**, **Suc-aT** (Fig. 5A–C, respectively) are indicative of a competitive mode of inhibition. The order of values obtained for the inhibition constants correlated well with those obtained from

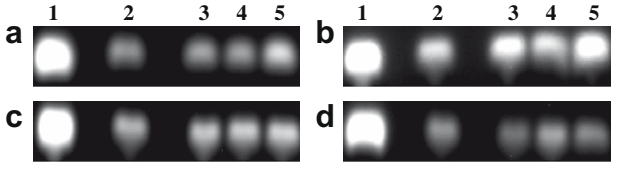

Figure 2. Agarose gel assay, RNase A and inhibitor concentrations 0.66 μM and 1.5 mM, respectively. Lane1: tRNA; Lane 2: tRNA and RNase A; Lane 3, 4 and 5: tRNA and RNase A with increasing concentration of nucleoside–dibasic acid conjugates; (a) **Oxa-aT**, (b) **Mal-aT**, (c) **Suc-aT**; (d) **Glu-aT**.

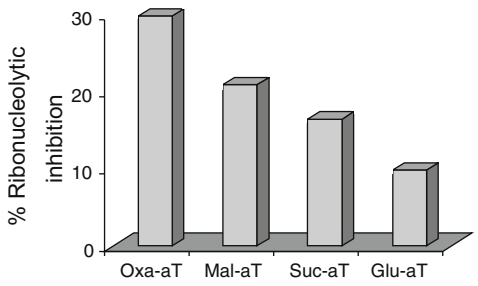

Figure 3. Ribonucleolytic inhibition of RNase A by nucleoside–dibasic acid conjugates. RNase A and compound concentration are 0.2 μM and 1 mM, respectively.

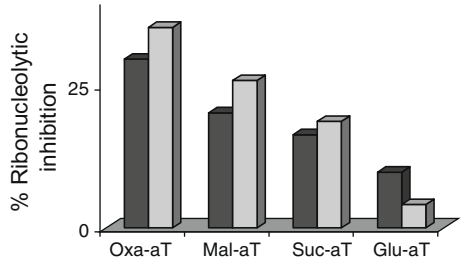

Figure 4. Comparative diagram for RNase A inhibition obtained from agarose gel (gray) and precipitation assay (black).

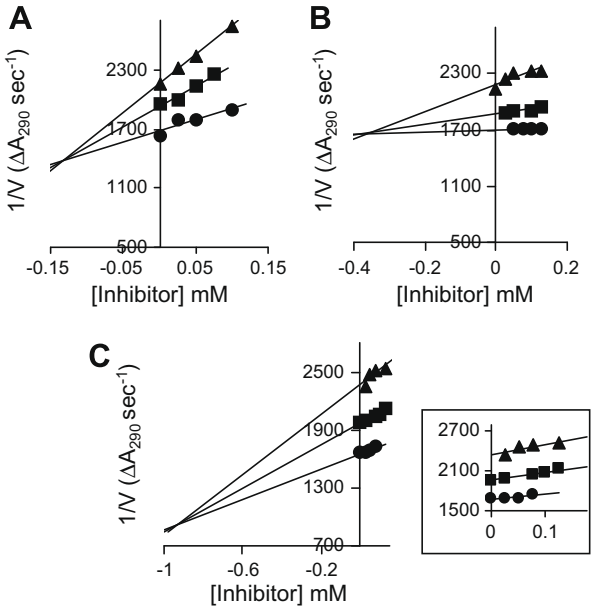

Figure 5. Dixon plots for inhibition of RNase A by (A) **Oxa-aT**: substrate concentrations: 250 μM (●), 200 μM (■) and 150 μM (▲); (B) **Mal-aT**: substrate concentrations: 238 μM (●), 190 μM (■) and 143 μM (▲); and (C) **Suc-aT**: substrate concentrations: 250 μM (●), 200 μM (■) and 150 μM (▲). RNase A concentration: 9 μM.

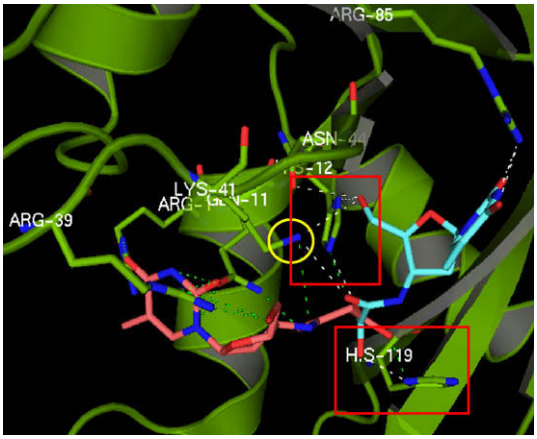

Figure 6. Docked conformations of **Oxa-aT** (cyan) and **Mal-aT** (orange) with RNase A (1FS3).

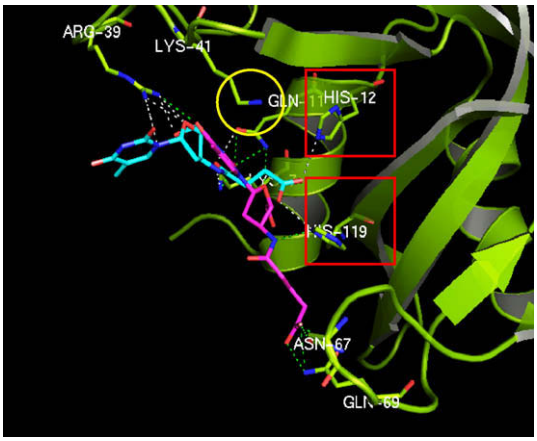

Figure 7. Docked conformations of **Suc-aT** (cyan) and **Glu-aT** (purple) with RNase A (1FS3).

the agarose gel and precipitation assay. In the kinetics experiment, **Glu-aT** did not show any inhibition (i.e., initial velocity in presence and absence of **Glu-aT** remain practically unchanged).

Keeping these results in mind, we further proceeded for protein–ligand docking studies to visualize the possible conformation of inhibitors in the protein–ligand complexes. From the docking experiments it was found **Oxa-aT** is in close proximity to the three P_1 site residues His-12, Lys-41 and His-119 (Fig. 6) and the pyrimidine (thymine) group occupied the B_1 site. The interaction of the carboxylic group with both His-12 and His-119 is expected to perturb the normal acid–base mechanism of RNase A thereby inhibiting its enzymatic activity. For **Mal-aT** the carboxylic group appears to interact with His-12 and His-119 residues in a more or less similar manner as for **Oxa-aT**. However, for this compound the nucleobase is far from the pyrimidine base recognition site, which is the probable reason for its weaker inhibition compared to **Oxa-aT**.

The docked conformation of compounds **Suc-aT** and **Glu-aT** (Fig. 7) showed that though the carboxylic group of **Suc-aT** was within hydrogen bonding distance with both His-12 and His-119 for **Glu-aT** only His-119 is within hydrogen bonding distance. Thus it was expected that **Suc-aT** perturbed the enzymatic activity more efficiently than **Glu-aT**. This may be attributed to the comparatively longer chain length of **Glu-aT**, that makes it unable to place its carboxylic group near the active site residues as observed for the other compounds but instead interacted with B_2 site residues.[21] Moreover, **Suc-aT** and **Glu-aT** did not interact with Lys-41 which forms a single hydrogen bond to stabilize the transition state during catalysis.[22] As a result they showed lower inhibitory activity compared to **Oxa-aT** and **Mal-aT**. These features corroborate the competitive mode of inhibition by this series of inhibitors.

3. Conclusion

Nucleoside–dibasic acid conjugates are shown to inhibit the ribonucleolytic activity of RNase A for the first time. The carboxylic group is expected to alter the microenvironment of the active site residues like their phosphate analogue. Although all compounds of this series contain one carboxylic group (exists in carboxylate form at the physiological *pH*), their inhibitory activity was found to be dependent on the length of dibasic acid part. With the increase of spacer length hydrophobicity of the molecules get increased as a result the binding of the molecules with the ionic active site becomes unfavorable which reflected from their K_i values. Thus the inhibitory activity for **Oxa-aT** was three fold greater than **Glu-aT**. Docking studies further substantiated these experimental observations. The major advantage of these compounds with substantial inhibitory properties is their low ionic character which is expected to facilitate transportation through biological membranes more

easily unlike nucleosides functionalized with phosphate or pyrophosphate.

The inhibitory properties in combination with their low ionic characters make these compounds suitable candidates for studies on their transportation through biological membranes in future.

4. Experimental

Bovine pancreatic RNase A, yeast tRNA, 2′,3′-cCMP, human serum albumin (HSA) were from Sigma–Aldrich. All other reagents were from SRL India. Column chromatographic separations were performed using silica gel (60–120 and 230–400 mesh). Solvents were dried and distilled following standard procedures. TLC was carried out on pre-coated plates (Merck silica gel 60, f_{254}), and the spots visualized with UV light or by charring the plates dipped in 5% H_2SO_4–MeOH solution or 5% H_2SO_4/vanillin/EtOH or 5% ninhydrin in MeOH solution. ^{1}H NMR (400 MHz) and ^{13}C NMR (100 MHz) spectra were recorded on a Bruker NMR spectrometer (δ scale). UV–vis measurements were made using a Perkin Elmer UV–vis spectrophotometer (Model Lambda 25). Concentrations of the solutions were determined spectrophotometrically using the following data: $\varepsilon_{278.5}$ (RNase A),[23] ε_{268} (2′,3′-cCMP)[24] are 9800 and 8500 M^{-1} cm^{-1}, respectively.

4.1. *N*-[2-Hydroxymethyl-5-(5-methyl-2,4-dioxo-3,4-dihydro-2*H*-pyrimidin-1-yl)-tetrahydro-furan-3-yl]-oxalamic acid (2)

A mixture of 3′-amino-2′,3′-dideoxy thymidine (**1**) (0.6 g, 1.2 mmol) and diethyl oxalate (0.5 g, 3.6 mmol) was stirred at 110 °C for 3 h. The excess diethyl oxalate was then removed by distillation. The oily residue thus obtained was treated with 4 N NaOH solutions and refluxed for 2 h. After cooling the reaction mixture it was filtered and the filtrate was acidified with 37% HCl and kept at 2 °C for 16 h. The aqueous layer was then evaporated under reduced pressure. Crude residues thus obtained were purified over silica gel using 30% methanol in chloroform as eluent to afford compound **2** (0.17 g, 45%); white hygroscopic solid. ^{1}H NMR: (DMSO-d_6): δ 1.75 (s, 3H), 2.13–2.30 (m, 2H), 3.59–3.75 (m, 3H), 3.88 (br s, 1H), 6.21 (t, J = 6.4 Hz, 1H), 7.75 (s, 1H). ^{13}C NMR (DMSO-d_6): δ 12.6, 37.4 (CH_2), 50.6, 61.2 (CH_2), 83.8, 84.7, 109.8 (C), 136.6, 150.8 (C), 164.2 (C), 171.9 (C), 174.6 (C). HRMS (ESI$^+$): m/z calcd for $C_{12}H_{15}N_3O_7Na$ [M+Na]$^+$: 336.0809; found: 336.0808.

4.2. *N*-[2-Hydroxymethyl-5-(5-methyl-2,4-dioxo-3,4-dihydro-2*H*-pyrimidin-1-yl)-tetrahydro-furan-3-yl]-malonamic acid (3)

A mixture of **1** (0.4 g, 0.8 mmol) and diethyl malonate (0.6 g, 3.5 mmol) was stirred at 150 °C for 3 h. The reaction mixture was worked up and hydrolyzed following the procedure described for **2** to afford compound **3** (0.13 g, 47%); white hygroscopic solid. ^{1}H NMR: (DMSO-d_6): δ 1.75 (s, 3H), 2.25–2.36 (m, 2H), 2.74 (br s, 1H), 3.14 (s, 1H), 3.66 (m, 2H), 3.80 (br s, 1H), 4.02 (br s, 1H), 6.27 (t, J = 6.4 Hz, 1H), 7.73 (s, 1H). ^{13}C NMR (DMSO-d_6): δ 12.6, 36.0 (CH_2), 40.0 (CH_2), 50.5, 61.3 (CH_2), 83.4, 83.8, 110.0 (C), 136.5, 150.8 (C), 164.2 (C), 172.0 (C), 186.7 (C). HRMS (ESI$^+$): m/z calcd for $C_1H_{17}N_3O_7Na$ [M+Na]$^+$: 350.0965; found: 350.0965.

4.3. *N*-[5-(5-Methyl-2,4-dioxo-3,4-dihydro-2*H*-pyrimidin-1-yl)-2-trityloxymethyl-tetrahydro-furan-3-yl]-succinamic acid (4)

Compound **1** (0.5 g, 1 mmol) was dissolved in dry DCM (5 ml), to this solution succinic anhydride (0.1 g, 1.0 mmol) and dry Et_3N (0.2 ml, 2.2 mmol) were added and stirred for overnight at room temperature. It was then diluted with DCM and extracted with 5% citric acid and then with brine.The organic layer was then evaporated under reduced pressure. Crude residues thus obtained were purified over silica gel using 5% methanol in chloroform as eluent to afford compound **4** (0.4 g, 68%); white solid; mp 82 °C (crystalized from DCM and MeOH). ^{1}H NMR: (DMSO-d_6): δ 1.43 (s. 3H), 2.12 (m, 1H), 2.26–2.39 (m, 5H), 3.15 (m, 1H), 3.26 (m, 1H), 3.86 (br s, 1H), 4.42–4.49 (m, 1H), 6.20 (t, J = 6.8 Hz, 1H), 7.23–7.38 (m, 15H), 7.52 (s, 1H), 8.29 (d, J = 7.6 Hz, 1H), 11.34 (s, 1H). ^{13}C NMR (DMSO-d_6): δ 12.2, 29.4 (CH_2), 30.4 (CH_2), 37.2 (CH_2), 49.5, 64.1 (CH_2), 83.5, 84.0, 86.8 (C), 110.0 (C), 127.6, 128.4, 128.7, 136.1, 143.9 (C), 150.8 (C), 164.1 (C), 171.4 (C), 174.3 (C). HRMS (ESI$^+$): m/z calcd for $C_{33}H_{33}N_3O_7Na$ [M+Na]$^+$: 606.2217; found: 606.2221.

4.4. *N*-[5-(5-Methyl-2,4-dioxo-3,4-dihydro-2*H*-pyrimidin-1-yl)-2-trityloxymethyl-tetrahydro-furan-3-ylcarbamoyl]-butyric acid (5)

Compound **1** (0.5 g, 1 mmol) was reacted with glutaric anhydride (0.1 g, 1.0 mmol) following the procedure described for **4** to afford compound **5** (0.4 g, 64%); white solid; mp 196 °C (crystallized from DCM and MeOH). ^{1}H NMR: (DMSO-d_6): δ 1.45 (s, 3H), 1.65 (m, 2H), 2.05–2.18 (m, 5H), 2.31 (m, 1H), 3.15–3.25 (m, 2H), 3.84 (br s, 1H), 4.47 (m, 1H), 6.17 (t, J = 6.4 Hz, 1H), 7.23–7.38 (m, 15H), 7.53 (s, 1H), 8.21 (d, J = 7.2 Hz, 1H), 11.33 (b, 1H). ^{13}C NMR (DMSO-d_6): δ 12.2, 21.0 (CH_2), 33.4 (CH_2), 34.8 (CH_2), 37.3 (CH_2), 49.1, 64.0 (CH_2), 83.5, 84.0, 86.8 (C), 110.0 (C), 127.5, 128.3, 128.7, 136.1, 143.9 (C), 150.7 (C), 164.1 (C), 171.9 (C), 174.6 (C). HRMS (ESI$^+$): m/z calcd for $C_{34}H_{35}N_3O_7Na$ [M+Na]$^+$: 620.2373; found: 620.2371.

4.5. *N*-[2-Hydroxymethyl-5-(5-methyl-2,4-dioxo-3,4-dihydro-2*H*-pyrimidin-1-yl)-tetrahydro-furan-3-yl]-succinamic acid (6)

Compound **2** (0.4 g, 0.7 mmol) was stirred with 50% TFA in DCM (7 ml) for 5 h at room temperature. The acid was then removed under reduce pressure. Crude residues thus obtained were purified over silica gel using 20% methanol in chloroform as eluent to afford compound **6** (0.2 g, 87%); white hygroscopic solid. ^{1}H NMR: (DMSO-d_6): δ 1.75 (s, 3H), 2.06–2.21 (m, 2H), 2.33 (m, 4H), 3.50–3.61 (m, 2H), 3.75 (s, 1H), 4.27 (br s, 1H), 5.16 (br s, 1H), 6.15 (t, J = 6.4 Hz, 1H), 7.78 (s, 1H), 8.44 (br s, 1H), 11.28 (br s, 1H). ^{13}C NMR (DMSO-d_6): δ 12.6, 29.5 (CH_2), 30.3 (CH_2), 37.4 (CH_2), 49.5, 61.6 (CH_2), 84.0, 85.5, 109.7 (C), 136.7, 150.8 (C), 164.2 (C), 171.6 (C), 174.2 (C). HRMS (ESI$^+$): m/z calculated for $C_{14}H_{19}N_3O_7Na$[M+-Na]$^+$: 364.1121; found: 364.1100.

4.6. 4-[2-Hydroxymethyl-5-(5-methyl-2,4-dioxo-3,4-dihydro-2*H*-pyrimidin-1-yl)-tetrahydro-furan-3-ylcarbamoyl]-butyric acid (7)

Compound **3** (0.3 g, 0.5 mmol) was deprotected following the procedure described for **6** to afford compound **7** (0.18 g, 94%); white hygroscopic solid. ^{1}H NMR: (DMSO-d_6): δ 1.76–1.77 (m, 5H), 2.09–2.26 (m, 6H), 3.51–3.62 (m, 2H), 3.73 (br s, 1H), 4.29 (br s, 1H), 6.15 (t, J = 6 Hz, 1H), 7.75 (s, 1H), 8.30 (s, 1H), 11.26 (br s, 1H). ^{13}C NMR (DMSO-d_6): δ 12.2, 21.0 (CH_2), 33.4 (CH_2), 34.8 (CH_2), 37.3 (CH_2), 49.1, 64.0 (CH_2), 84.0, 86.8 (C), 110.0 (C), 136.1, 150.7 (C), 164.1 (C), 171.9 (C), 174.6 (C). HRMS (ESI$^+$): m/z calcd for $C_{15}H_{21}N_3O_7Na$ [M+Na]$^+$: 378.1277; found: 378.1250.

4.7. Agarose gel-based assay

Inhibition of RNase A by all nucleoside–dibasic acid conjugates was checked qualitatively by the degradation of tRNA in an agarose gel. In this method, 20 μl of RNase A (0.66 μM) (in TAE buffer) was mixed with 10, 15 and 20 μl of the compounds (1.5 mM) to a final

volume of 50 μl and the resulting solutions were incubated for 6 h at 37 °C. 20 μl aliquots from incubated mixtures were then mixed with 20 μl of tRNA solution (5.0 mg/ml) and 10 μl of sample buffer (containing 10% glycerol and 0.025% bromophenol blue). The mixture was then incubated for another 30 min. A volume of 15 μl from each solution were extracted and loaded onto a 1.1% agarose gel. The gel was run in 0.04 M Tris–acetic acid–EDTA (TAE) buffer (pH 8.0). The undegraded tRNA was visualized by ethidium bromide staining under UV light. Gel images were captured on a KODAK Gel Logic 200 imaging system and relative intensities of the bands were estimated using Kodak Molecular imaging software.

4.8. Precipitation assay

Inhibition of the ribonucleolytic activity of RNase A was quantified by the precipitation assay as described by Bond.[25] In this method 10 μl of RNase A (2 μM) was mixed with 50 μl of each nucleoside–dibasic acid conjugate (2 mM) to a final volume of 100 μl and incubated for 2 h at 37 °C. A 20 μl aliquot of the resulting solutions from the incubated mixtures were then mixed with 40 μl of tRNA (5 mg/ml), 40 μl of Tris–HCl buffer of pH 7.5 containing 5 mM EDTA and 0.5 mg/ml HSA. After incubation of the reaction mixture at 25 °C for 30 min, 200 μl of ice–cold 1.14 (*N*) perchloric acid containing 6 mM uranyl acetate was added to quench the reaction. The solution was then kept in ice for another 30 min and centrifuged at 4 °C at 12,000 rpm for 5 min. A 100 μl aliquot of the supernatant was taken and diluted to 1 ml. The change in absorbance at 260 nm was measured and compared to a control set.

4.9. Inhibition kinetics

The inhibition of RNase A by **Oxa-aT**, **Mal-aT**, **Suc-aT** and **Glu-aT** was assessed individually by a spectrophotometric method as described by Anderson et al.[24]The assay was performed in oligovinylsulfonic acid free[26] 0.1 M Mes–NaOH buffer, pH 6.0 containing 0.1 M NaCl using 2′,3′-cCMP as the substrate. The inhibitor concentration was ranged from 0 to 100 μM and the substrate concentration was used from 150 to 250 μM. The RNase A concentration was 9 μM. The inhibition constants (K_i) were determined from initial velocity data. The reciprocal of initial velocity was plotted against the inhibitor concentration (Dixon Plot) according to the equation:

$$\frac{1}{v} = \frac{K_m}{V_{max}[S]K_i}[I] + \frac{1}{V_{max}}\left[1 + \frac{K_m}{[S]}\right] \quad (1)$$

where v is the initial velocity, [*S*] the substrate concentration, [*I*] the inhibitor concentration, K_m the Michaelis constant, K_i the inhibition constant and V_{max} the maximum velocity.

4.10. Docking studies of the compounds with RNase A (1FS3)

The crystal structure of RNase A (PDB entry 1FS3) was downloaded from the Protein Data Bank.[27] The 3D structures of the nucleoside–dibasic acid conjugates were generated by Sybyl6.92 (Tripos Inc., St. Louis, USA) and their energy-minimized conformations were obtained with the help of the TRIPOS force field using Gasteiger-Hückel charges with a gradient of 0.005 kcal/mole. The *FlexX* software as part of the Sybyl suite was used for docking of the nucleoside–dibasic acid conjugates with RNase A. *PyMol*[28] was used for visualization of the docked conformations.

Acknowledgments

J.D. thanks CSIR, India for a fellowship. S.D. and T.P. are grateful to the Department of Science and Technology (DST), New Delhi, India, for financial support.

Supplementary data

Supplementary data associated with this article can be found, in the online version, at doi:10.1016/j.bmc.2009.08.018.

References and notes

1. Kurachi, K.; Davie, E. W.; Strydom, D. J.; Riordan, J. F.; Vallee, B. L. *Biochemistry* **1985**, *24*, 5494.
2. Strydom, D. J.; Fett, J. W.; Lobb, R. R.; Alderman, E. M.; Bethune, J. L.; Riordan, J. F.; Vallee, B. L. *Biochemistry* **1985**, *24*, 5486.
3. Rybak, S. M.; Hoogenboom, H. R.; Meade, H. M.; Raus, J. C. M.; Schwartz, D.; Youle, R. J. *Proc. Natl. Acad. Sci. U.S.A.* **1992**, *89*, 3165.
4. Loverix, S.; Steyaert, J. *Curr. Med. Chem.* **2003**, *10*, 779.
5. Rosenberg, H. F.; Domachowske, J. B. *Methods Enzymol.* **2001**, *341*, 273.
6. Russo, N.; Acharya, K. R.; Shapiro, R. *Methods Enzymol.* **2001**, *341*, 629.
7. Raines, R. T. *Chem. Rev.* **1998**, *98*, 1045.
8. Nogués, M. V.; Vilanova, M.; Cuchillo, C. M. *Biochim. Biophys. Acta* **1995**, *1253*, 16.
9. Witzel, H.; Barnard, E. A. *Biochem. Biophys. Res. Commun.* **1962**, *7*, 295.
10. Yakovlev, G. I.; Mitkevich, V. A.; Makarov, A. A. *Mol. Biol.* **2006**, *40*, 867.
11. Maiti, T. K.; De, S.; Dasgupta, S.; Pathak, T. *Bioorg. Med. Chem.* **2006**, *14*, 1221.
12. Leonidas, D. D.; Maiti, T. K.; Samanta, A.; Dasgupta, S.; Pathak, T.; Zographos, S. E.; Oikonomakos, N. G. *Bioorg. Med. Chem.* **2006**, *14*, 6055.
13. Samanta, A.; Leonidas, D. D.; Dasgupta, S.; Pathak, T.; Zographos, S. E.; Oikonomakos, N. G. *J. Med. Chem.* **2009**, *52*, 932.
14. Roy, B.; Dutta, S.; Chowdhary, A.; Basak, A.; Dasgupta, S. *Bioorg. Med. Chem. Lett.* **2008**, *18*, 5411.
15. Wrobel, J.; Green, D.; Jetter, J.; Kao, W.; Rogers, J.; Perez, M. C.; Hardenburg, J.; Deecher, D. C.; Lopez, F. J.; Arey, B. J.; Shen, E. S. *Bioorg. Med. Chem.* **2002**, *10*, 639.
16. Leitner, N. K. V.; Berger, P.; Legube, B. *Environ. Sci. Technol.* **2002**, *36*, 3083.
17. Bartra, M.; Romea, P.; Urpí, F.; Vilarrasa, J. *Tetrahedron* **1990**, *46*, 587.
18. Herdewijin, P.; Balzarini, J.; Baba, M.; Pauwels, R.; Van Aerschot, A.; Janssen, G.; De Clercq, E. *J. Med. Chem.* **1988**, *31*, 2040.
19. Balint, J.; Egri, G.; Czugler, M.; Schindler, J.; Kiss, V.; Juvancz, Z.; Fogassy, E. *Tetrahedron: Asymmetry* **2001**, *12*, 1511.
20. Claussen, R. C.; Rabatic, B. M.; Stupp, S. I. *J. Am. Chem. Soc.* **2003**, *125*, 12680.
21. Toiron, C.; Gonzalez, C.; Bruix, M.; Rico, M. *Protein Sci.* **1996**, *5*, 1633.
22. Gerlt, J. A.; Gassman, P. G. *Biochemistry* **1993**, *32*, 11943.
23. Sela, M.; Anfinsen, C. B. *Biochim. Biophys. Acta* **1957**, *24*, 229.
24. Anderson, D. G.; Hammes, G. G.; Walz, F. G. *Biochemistry* **1968**, *7*, 1637.
25. Bond, M. D. *Anal. Biochem.* **1988**, *173*, 166.
26. Smith, B. D.; Soellner, M. B.; Raines, R. T. *J. Biol. Chem.* **2003**, *278*, 20934.
27. Berman, H. M.; Westbrook, J.; Feng, Z.; Gilliland, G.; Bhat, T. N.; Weissig, H.; Shindyalov, I. N.; Bourne, P. E. *Nucleic Acids Res.* **2000**, *28*, 235.
28. DeLano, W. L. The PyMOL Molecular Graphics System, DeLano Scientific, San Carlos, CA, 2006. USA. http://pymol.sourceforge.net/.